View metadata, citation and similar papers at core.ac.uk
brought to you by CORE
provided by Apollo

Segmented packed beds for improved thermal energy storage performance

Joshua D. McTigue[1,*] and Alexander J. White[1]

[1]Cambridge University Engineering Department, Trumpington Street, Cambridge, CB2 1PZ
[*]jdm70@cam.ac.uk

Abstract: A scheme for bulk electricity storage known as Pumped Thermal Energy Storage (PTES) is described. PTES uses a heat pump during the charging phase to create a hot and a cold storage space. During discharge, these thermal stores are depleted using a heat engine. This version of PTES uses packed beds (or pebble beds) as the energy store. A relatively new design feature which involves segmenting the packed beds is introduced. Various thermodynamic benefits can be achieved by reservoir segmentation, such as reduced pressure losses and increased energy stored per cycle. This report includes modelling of the storage phases, and it is found that segmentation can reduce the thermal equilibration losses that occur. A simple economic model of the PTES system is introduced so that multi-objective optimisation of efficiency and capital costs can be carried out. Sensitivity to the economic factors is briefly explored. The results show that cold packed beds in particular benefit from being segmented.

1. Introduction

The 2009 EU Renewables Directive committed the UK to generating 15% of its final energy consumption from renewable sources by 2020. In 2014 the UK achieved a value of 7.0% [1], indicating that substantial deployment of renewable technologies may occur in the next few years. Renewable energy technologies have the potential to reduce the consumption of fossil fuels and the environmental and health concerns that arise from their use. However, wind and solar energy in particular suffer from intermittent and uncertain outputs which may compromise their integration with the electrical grid and their cost effectiveness.

Energy storage, interconnection, and demand side management have the potential to combat these problems, and it is widely accepted that energy storage will form an essential component in future energy systems [2]. In the UK, for example, it is estimated that over the next few decades integration of intermittent sources into the power infrastructure will require storage capacities of the order of hundreds of GWh an order of magnitude greater than current capacity [3].

A significant proportion of the UKs renewable energy is likely to be provided by offshore wind farms with around 4.5 GW currently installed [1]. As a result, it will be necessary to consider the development of energy storage technologies in off-shore or coastal applications.

2. Pumped thermal electricity storage (PTES)

A number of thermal energy storage (TES) systems have now been proposed for large-scale storage of electricity at either the distribution or transmission level. The present paper is concerned with a form of TES that has both hot and cold packed-bed thermal stores and is known as Pumped Thermal Electricity Storage (PTES). Several independent patents for similar technologies emerged around the same time. The particular variant described here is based mainly on that described in [4] by Isentropic Ltd.

During the charging phase, PTES acts as a heat pump, using electrical energy to move energy from the cold reservoir (CR) to the hot reservoir (HR), thereby creating a temperature difference. Electrical energy is thus converted to thermal energy which resides in the packed-bed thermal stores (see figure 1a)). When electricity is required, the PTES system discharges by operating as a heat engine, returning heat from the hot to the cold store and recovering electrical energy in the process.

The main metrics for assessing energy storage devices are its roundtrip efficiency, and the capital cost per MW and per MWh of storage. PTES benefits from having a relatively high energy density, which suggests a small plant footprint and low cost per MW h: the estimated energy density of a typical PTES plant is around 50 kWh m^{-3} compared to 10 kWh m^{-3} for CAES [5]. PTES is not restricted geographically and could therefore be easily implemented in areas where there is less potential for Pumped Hydro such as in coastal regions.

Accurate evaluation of the above metrics requires detailed computational models of each component. Compressors and expanders are modelled as reciprocating devices, as proposed by Isentropic, with polytropic efficiencies, heat leakage factors and pressure loss factors taken into account as in [5]. The roundtrip efficiency is particularly sensitive to the value of the polytropic efficiency and heat leakage factor. For instance, a 2% drop in polytropic efficiency typically leads to a 4% drop in roundtrip efficiency [6].

Careful design of the thermal stores can reduce the exergetic losses such that they are relatively small compared to the compressors and expanders. This paper will focus on some of the thermodynamic behaviour of the packed-bed thermal reservoirs and will introduce a new design approach which involves segmenting the thermal reservoirs, a concept which was under development by Isentropic Ltd [7]. A multi-objective optimisation algorithm is then used to optimise a PTES system with segmented packed beds. A simple economic model is developed such that the optimisation can consider economic factors as well as thermodynamic performance.

3. Thermal reservoir modelling

In PTES, thermal energy is stored in packed beds: cylindrical pressure vessels filled with pebbles which in this case are composed of magnetite (Fe_3O_4). Heat or cold is transferred to and from the packed bed by passing a gas (argon) through the pebbles.

The performance of the thermal reservoirs is controlled by a number of heat transfer mechanisms, including convective heat transfer between the gas and solid, conduction along the packed bed, and heat leakage from walls of the container. Each of these processes contributes to exergetic losses, that is, a reduction in the energy that can be recovered from the packed beds and converted to useful work.

The model used to quantify the heat transfer processes is based on the well-established Schumann model [8], which assumes that the flow is one dimensional, and that the heat transfer is

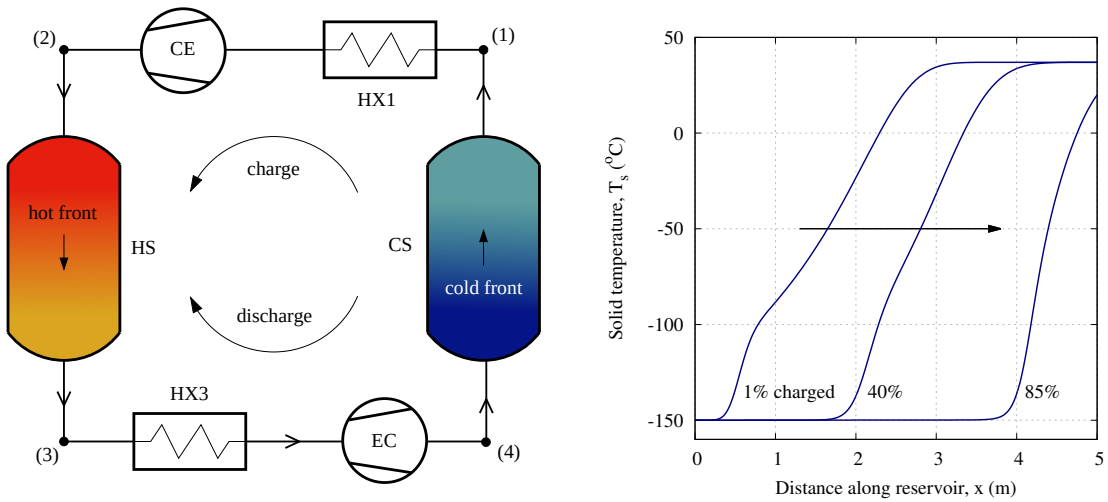

(a) (b)

Fig. 1.
a) Layout of PTES system. Key: HR/CR hot/cold reservoir; CE/EC reversible compressor-expanders; HX1/HX3 heat exchangers
b) Typical thermal fronts in a cold packed bed during charge. Profiles are shown at 1%, 40% and 85% through the charging phase

limited by surface effects (i.e. the internal thermal resistance of the particles is negligible). The numerical model includes the full unsteady equations but, due to the low heat capacity of the gas per unit volume compared to that of the solid, the gas unsteady terms are almost always negligible. By assuming steady flow (for clarity of exposition only) through an infinitesimal layer of a packed bed the energy equations for the gas and solid phases can be derived. The various assumptions and derivation are presented in [8, 9, 10]. The energy equations can be written in terms of the gas and solid temperatures, T_g and T_s, respectively, to give:

$$\frac{\partial T_g}{\partial x} = \frac{T_s - T_g}{\ell} \tag{1}$$

and

$$\frac{\partial T_s}{\partial t} = \frac{T_g - T_s}{\tau} + \alpha \frac{\partial^2 T_s}{\partial x^2} + \beta \left(T_0 - T_s\right) \tag{2}$$

where

$$\ell = \frac{1}{\mathrm{St}\left(1-\varepsilon\right) S_v} \tag{3}$$

$$\tau = \frac{\rho_s c_s}{\mathrm{St} c_p G S_v} \tag{4}$$

In these expressions, G is the mass flow rate per unit area; $\mathrm{St} = h/(Gcp)$ is the Stanton number (obtained from correlations in [11]); S_v is the particle surface-to-volume ratio which is $6/d_p$ for spherical particles; ε is the void fraction; $\alpha = k_{\text{eff}}/\rho_s c_s\,(1-\varepsilon)$ is the effective thermal diffusivity arising due to conduction; and $\beta = 4U_s/\left(\rho_s c_s\,(1-\varepsilon)\,D\right)$ is related to heat leakage from the walls. For further details of this particular thermal model, its justifications, and a discussion of the influence of each parameter, the reader is directed to Refs. [6, 8, 9, 10].

Several refinements are made to this model, including unsteady gas accumulation and temperature dependence of the solid and gas properties. The gas density varies with the ideal gas law, the gas viscosity follows Sutherland's Law, and the gas isobaric heat capacity does not vary over the temperature range of interest [12]. These additions generally have only a small effect, with the exception of the variation of the solid heat capacity c_s which significantly affects thermal front shapes and therefore the losses [10]. By extending the Schumann model to incorporate these factors allows the subtle, time-varying behaviour of the packed beds to be captured. Further details and a semi-analytical approach to solving these equations is described in [9].

Typical thermal fronts in a cold packed bed are shown in figure 1b). The reservoir is shown during charge, and as cold is transferred from the gas to the solid the fronts progress along the length of the reservoir.

A number of irreversible processes act to reduce the exergetic efficiency of the packed beds, and are termed *availability* losses. These losses are described below and the way in which they are defined and affected by design parameters is explored in greater detail in [6].

(i) Thermal losses occur as the result of a finite temperature difference between the gas and solid. Steeper thermal fronts lead to increased thermal losses as a result of greater temperature differences and a reduced area for heat transfer.

(ii) Pressure losses arise due to frictional effects, and the pressure gradient can be calculated from Ergun's equation. There is an inherent trade-off between thermal losses and pressure losses. For instance, long packed beds and small particles will lead to small thermal losses at the expense of frictional effects.

(iii) Exit losses occur as the thermal fronts approach the exit of the reservoir, as can be seen from the 85% curve of figure 1b). For instance, if this occurs during the charge of a hot store, the hot exit gas is cooled in a heat exchanger which leads to a loss in availability.

(iv) Heat leakage occurs through the side walls and from the top and bottom of the reservoir. The losses depend on various factors such as the size of the packed beds, the thickness of the insulation and, to a lesser extent, the convective heat transfer coefficients on the inner and outer wall (which in turn depend on the wall Reynolds and Grashof numbers, respectively).

(v) Conductive losses are due to the dissipative process of conduction between the pebbles. This loss depends on the value of the effective conductivity between particles which is fairly low ($\sim$0.5 W/mK) during charging and discharging periods. However, during non-operational periods, or "storage phases", the equilibration of the thermal front due to conduction could lead to significant availability losses, depending on the duration of storage. The entropy generation rate due to conduction can be found from consideration of the first and second law of thermodynamics. Such an analysis indicates that conductive losses are largest where the thermal front is steep and the temperature is low. Continued heat leakage during this time may lead to thermal gradients across the radius, or top and bottom, of the store, which may exacerbate conductive losses.

4. Segmentation of thermal reservoirs

Crandall and Thatcher [13] proposed segmentation as a way to maintain thermal stratification in packed beds for solar air heating applications. More recently, layered stores have been developed for PTES systems by Isentropic Ltd [7] to exploit a variety of other benefits during operational periods and storage periods. The present paper discusses the impact of segmentation on losses during the storage phase, and investigates the inclusion of segmented stores in a PTES system.

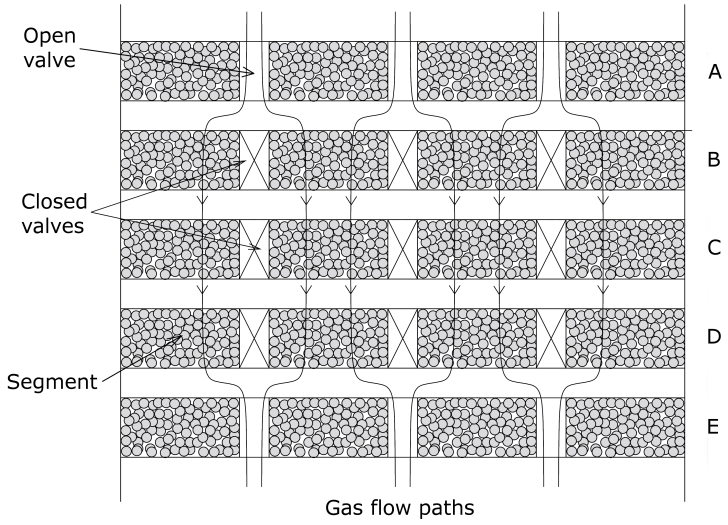

Fig. 2. *Schematic of a segmented packed bed. Gas follows the path of least frictional resistance. The gas flows through the open valve in the segment A, and is then diverted through the packed bed in segments BD due to the closed valves. Once the segment B is sufficiently charged, the valve may be opened such that gas passes through only segments C and D.*

As described in [7] there are several ways in which the beds may be segmented and controlled. One possible configuration is illustrated schematically in figure 2. By operating the stores in such a way that gas only passes through the segments where the thermal front is present pressure losses may be reduced. For instance, consider a hot packed bed at the start of charge. Hot inlet gas would enter the first segment and, once the gas was cooled, it would be diverted around the remaining segments, thereby avoiding the pressure loss that would otherwise be incurred. Once the thermal front had passed through the first segment, gas would be diverted around this segment and enter the second segment. The segments that the gas flows through can be controlled by valves within the segment: the gas will take the path of least resistance and will pass through the valve if it is open, or through the packed bed if it is closed. The reduction of pressure losses is most significant in reservoirs where the gas density is low and pressure losses are more significant, such as in cold stores.

Figure 3a) shows the trade-off between pressure losses and thermal losses that occurs as the particle diameter is varied in packed beds with either one segment or 32 segments. Segmenting the reservoirs clearly reduces the pressure losses, with a small increase in thermal losses arising due to the process of segments being switched on and off. Segmentation thereby shifts the optimal particle size to smaller values. Smaller particles also correspond to steeper thermal fronts [6], such that utilisation of the packed bed increases. In figure 3b) the cycling frequency of three segmented

cold reservoirs is varied illustrating the expected trade-off between efficiency and the available energy that is returned during the discharging phase. (The returned available energy is equal to the maximum flux of exergy that could be transferred to the store during charge [9] multiplied by the round-trip efficiency of the storage. Therefore, the returned available energy takes the loss generating mechanisms described in section 3 into account [6]). The optimal particle size has been evaluated for each number of segments, and is used in this calculation. By segmenting the stores and using smaller particles reservoir performance is improved.

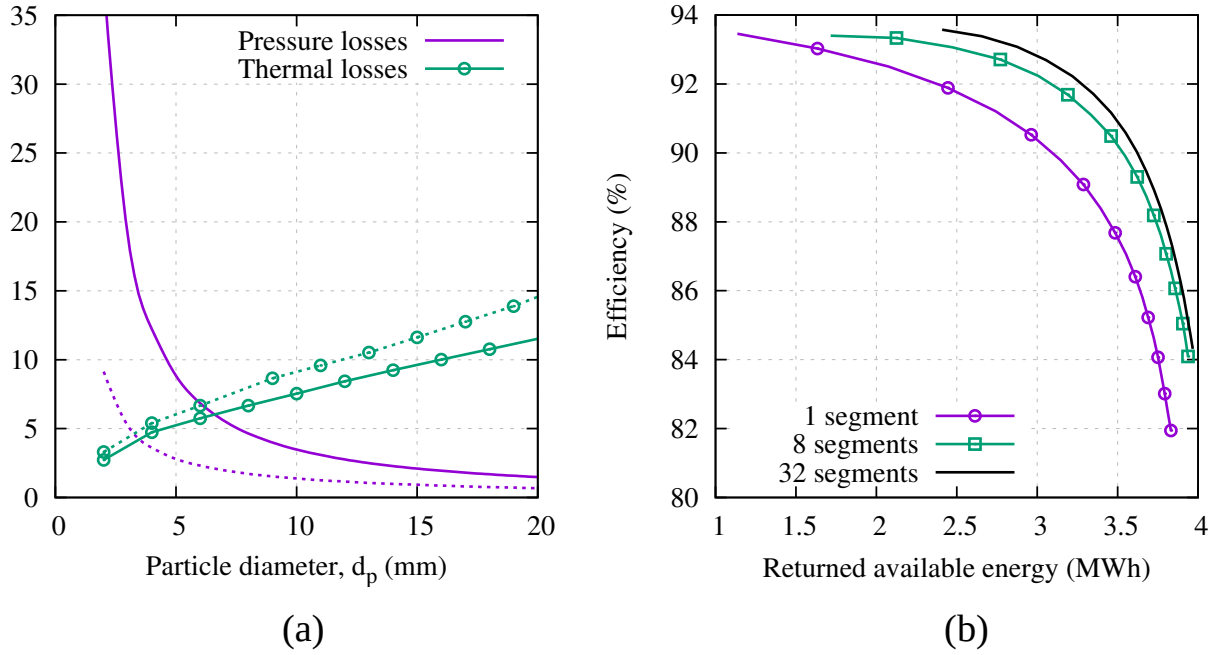

Fig. 3. *Availability losses in cold segmented packed-beds: the beds are charged to -150°C and discharged to 37°C. The pressure is 1.05 bar, the mass flow rate is 13.7 kg s^{-1}, and the charging duration is 6 hours.*
a) Thermal and pressure availability losses during cyclic operation of a cold packed bed with one segment (solid lines) and 32 segments (dashed lines).
b) Trade-off between efficiency and returned available energy in cold packed beds each with optimal particle diameter which is 10 mm for one segment, 8 mm for 8 segments and 7 mm for 32 segments. The charging frequency is varied between 0.3 and 0.95 to generate the curves.

Availability losses occur during the storage phase, in the form of heat leakage and conductive losses. A simple model of the storage phase is developed to demonstrate packed bed behaviour during storage. It is assumed that the gas and solid have the same temperature, T, and that the only heat transfer processes that occur are due to conduction and heat leakage.

$$\frac{\partial T}{\partial t} = \alpha \frac{\partial^2 T}{\partial x^2} + \beta \left(T - T_0\right) \tag{5}$$

Where $\alpha = k_{\text{eff}} / \rho_s c_s \left(1 - \varepsilon\right)$ and $\beta = 4U_s / \left(\rho_s c_s \left(1 - \varepsilon\right) D\right)$, and k_{eff} is the effective conductivity and U_s is the overall heat transfer coefficient of the side walls. The analytical solution to

this equation for an initially linear thermal front in a packed bed with adiabatic boundaries is expressed as a Fourier series and is solved by separation of variables. For more detailed calculations (i.e. segmented stores, with a heat flux from the top and bottom of the thermal store, and radiation between the segments), the Crank-Nicolson method is employed.

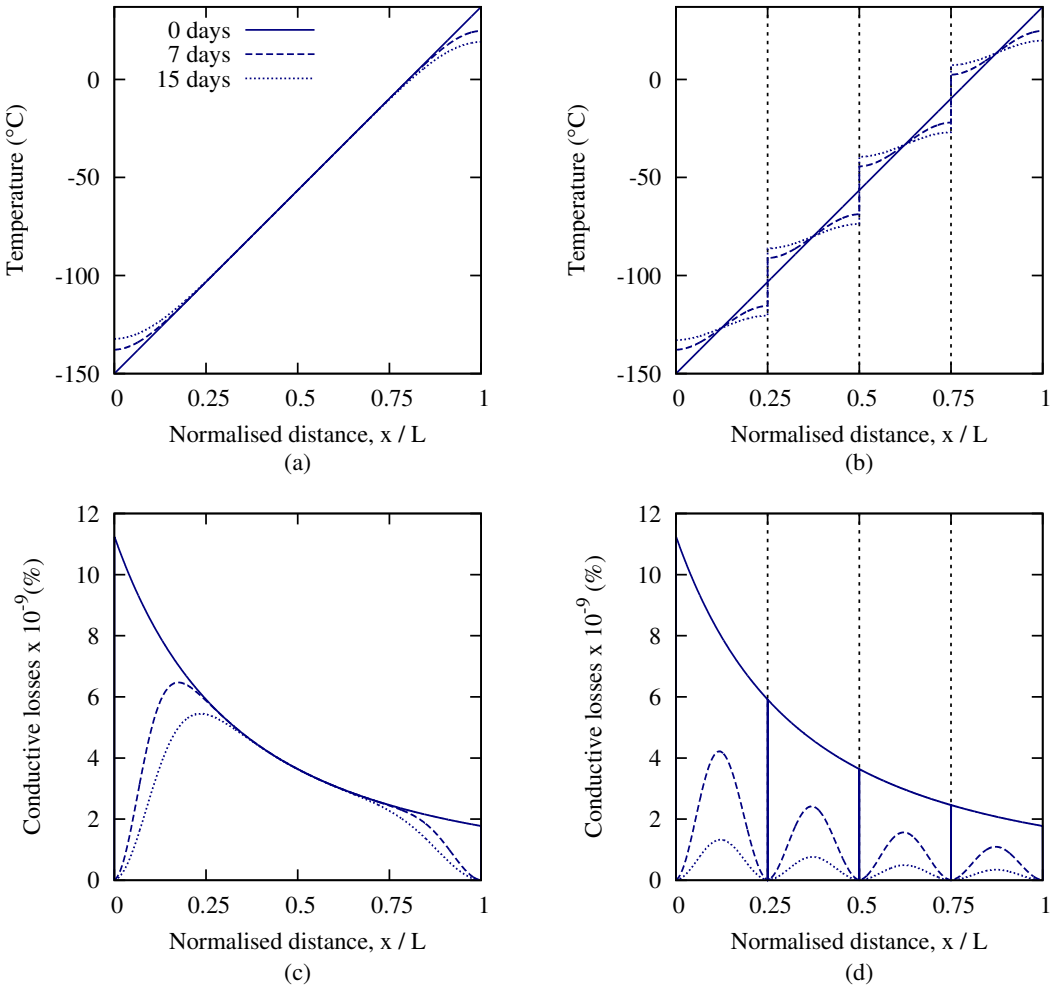

Fig. 4. *Conductive storage losses in cold segmented packed beds with adiabatic boundaries.*
a) Temperature profile in an unsegmented cold reservoir
b) Temperature profile in a cold reservoir with four segments
c) Instantaneous conductive losses in an unsegmented cold reservoir
d) Instantaneous conductive losses in a cold reservoir with four segments

Figures 4a) and 4b) shows thermal equilibration in cold packed beds with one and four segments. In this example, a linear front crosses the full reservoir, and the boundaries and walls are adiabatic ($\beta = 0$), as are the boundaries between segments. For figures 4a) and 4b), as the thermal front equilibrates, both temperature profiles have the same energy content. However, the stepped profile of the segmented store has a greater *available* energy content.

The conductive loss that is generated at each location along the reservoir is shown in figures 4c) and 4d) at three points in time. The largest conductive losses are generated at points where the

thermal gradient is steepest and where the temperature is lowest. Conductive losses decrease at the boundaries first, where the thermal gradient is reduced by conduction. The segmented case has the same conductive loss generation as the unsegmented case at zero days. However, the greater number of boundaries means that the thermal gradient is reduced at more points in the segmented reservoir. As a result, the total conductive loss at each time-step is less than in the unsegmented reservoir: the total area under each curve for the segmented reservoir is always equal or less than the corresponding unsegmented curve.

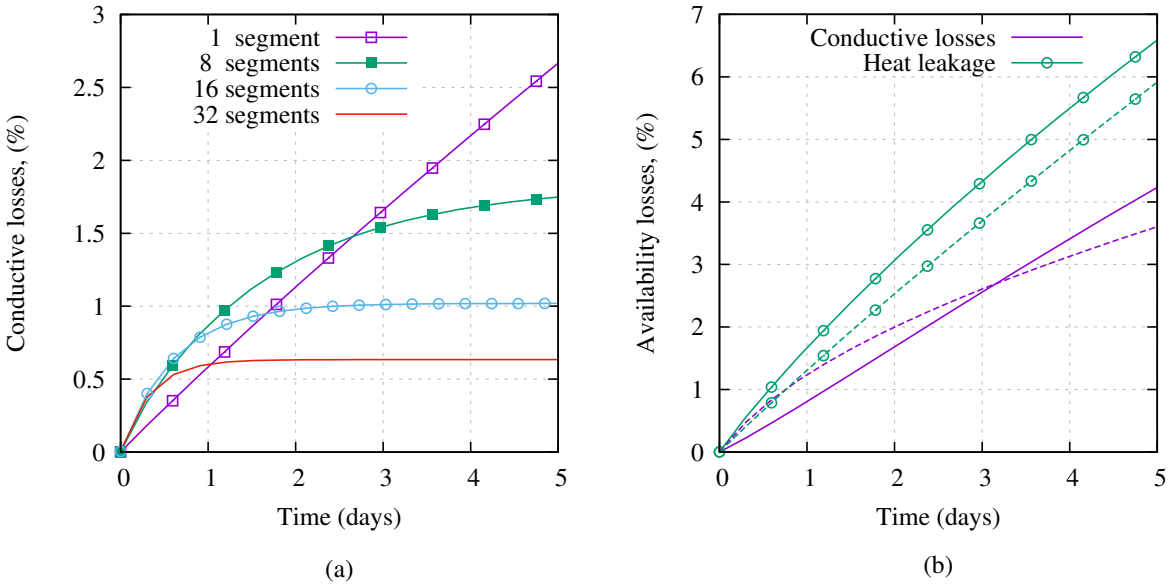

Fig. 5. *Availability storage losses in cold segmented packed beds with the thermal front in the final segment only.*
a) Conductive losses for adiabatic, fully insulated reservoirs
b) Conductive and heat leakage losses for packed beds with one (solid line) and 16 segments (dashed line)

In reality, at the end of charging the thermal front will not cross the full length of the reservoir and the front's position depends on a number of factors such as the cycle frequency, particle size and number of segments. As a result, the simplest and fairest way to judge the behaviour of segmented reservoirs during the storage phase is to use the thermal front position that would occur if that reservoir had been optimised. For a segmented packed bed the optimal design (minimum availability losses) will result in a thermal front that approximately crosses only the final segment. Therefore, the simplified thermal profile is given by a linear profile in the final segment, while all other segments are fully charged. Figure 5a) shows how the conductive losses vary with time for different numbers of segments for the case where $k_{\text{eff}} = 0.5$ W / mK. (The effective conductivity is subject to some uncertainty, but estimates suggest that this value is realistic). Conductive losses increase more quickly in packed beds with more segments due to the steeper thermal gradient in the final layer. However, over a longer period of time the benefit of segmenting the reservoirs is obvious: for instance, conductive losses in a reservoir with 32 layers are around one fifth of those in an unsegmented store.

Heat leakage also occurs during the storage phase and the interplay between conductive losses

and leakage should be considered. Figure 5b) illustrates how conductive and leakage losses develop with time in a cold segmented packed bed. The leakage loss includes leakage from the side walls and the top and bottom of the reservoir, all with an overall heat transfer coefficient of $U = 0.16$ W / mK (this value is consistent with the stores described in [6]). It is notable that conductive losses do not level off to the same extent as in figure 5a), and are in fact much larger. Heat leakage from the reservoir ends generate additional thermal gradients which are then eroded by conduction.

In this example, segmentation provides little benefit during the storage phase as a consequence of the interplay with heat leakage. However, segmentation can significantly reduce conductive losses providing that the packed beds are sufficiently insulated. Furthermore, segmentation will have the greatest benefit in systems where it is anticipated that storage phases may last a number of days.

5. Economic modelling of PTES

Holistic optimisation of the PTES system should consider not only technical issues, but also economic factors. A sophisticated economic model would take into account capital costs, operation and maintenance costs and future energy markets; electricity prices, subsidies, taxes etc. Furthermore, energy storage has various different revenue streams (the most commonly discussed is arbitrage, which could lead to 'self-cannibalisation' of its own market), and it is unclear how profitable these streams are, how payments will be organised, and how the market will be regulated. Inclusion of these details would provide information about the feasibility and/or profitability of the system, and the design and mode of operation that would achieve this.

The inherent uncertainty of these factors (and other externalities) suggests that any judgements about the profitability of an energy storage system are meaningless without undertaking comprehensive sensitivity analysis. The uncertainty and complexity can be reduced by developing simpler economic models although these may be unable to capture the true nature of the problem and still be quite uncertain (see below).

The current paper does not aim to evaluate how feasible PTES system may be. Instead, economic factors are used to compare different designs to evaluate which may be the most feasible design. Consequently, it is the relative magnitude of the economic factors that are of importance, rather than the absolute values themselves. The simplest economic metric to use is the capital cost (which has been normalised, since giving it a value may be misleading and distracting). Whilst this approach neglects the complexities discussed above, and other economic factors are likely to influence the design, capital cost is the most straight-forward starting place.

The capital cost is modelled by considering the material requirements of each component and the packed bed cost is given by

$$C_{\text{bed}} = k_p V_p + k_i V_i + k_{\text{PV}} V_{\text{PV}} \left(P_0 + \Delta P\right) \tag{6}$$

Where V refers to the volume of a material and k is the material cost per unit volume. The subscripts p, i, and PV refer to the packing material (magnetite), insulation and pressure vessel, respectively. The pressure vessel cost is assumed to be proportional to the volume and the pressure difference across the walls ΔP. The additional term P_0 is the ambient pressure and allows for unpressurised vessels. For segmented stores, the pressure vessel volume includes additional volume which is required for bypass flow and inter-segment gaps. The size of these gaps may be

calculated from pressure loss considerations. Thus, segmentation entails a cost penalty. However, the extra costs of valving, sensing and control which are necessary for segmentation to work are not included.

The reciprocating compressor/expander capital cost is given by

$$C_r = k_r \beta \dot{V} \tag{7}$$

Where k_r is the capital cost per volumetric flow rate $\dot{V}$, per pressure ratio β. The total capital cost is then given by

$$C_{\text{cap}} = C_{\text{bed}}^{\text{HOT}} + C_{\text{bed}}^{\text{COLD}} + 2C_r \tag{8}$$

The expression for capital cost contains four uncertain parameters k, and table 1 shows these cost factors which are taken from data in the literature, and by using the CES EduPack Materials Selector Software [14]. Preliminary analysis suggests that the capital cost is dominated by the pressure vessel and the reciprocating devices. The values of k_{PV} and k_r also happen to be the most uncertain such that k_p and k_i are likely to have a negligible impact and can be considered to be constant. Since only the relative magnitudes of the cost factors are important in this study, and only k_{PV} and k_r are of interest, sensitivity to economic uncertainty can be explored by varying k_r and keeping k_{PV} fixed. Thermo-economic optimisation is undertaken in the next section and this approach is used to observe the impact of economic uncertainty on optimal PTES designs.

Table 1 Cost factors used in the economic analysis

Component		Cost factor
k_p	(£/m^3)	1400
k_i	(£/m^3)	1950
k_{PV}	(£/m^3·bar)	200
k_r	(£/m^{3}s^{-1})	8000

6. Thermo-economic optimisation

Previous work has included multi-objective thermodynamic optimisation of a PTES system where the efficiency, power density and energy density were maximised [6]. Energy density was used as a proxy for economic factors. This work did not use segmented stores, nor did it include conductive losses, heat leakage or storage periods. The current paper will carry out optimisation of segmented packed beds integrated with a PTES system and including economic factors.

The design space for a PTES system is multi-dimensional and is possibly multi-modal and disjoint due to the large number of design variables, objectives and constraints. This makes optimisation by systematic parameter variation a complex task. A stochastic optimisation algorithm has therefore been applied to identify promising designs. The routine chosen for this purpose is a 'non-dominated sorting genetic algorithm' (NSGA-II) as described in [15]. Like other stochastic methods, this is well suited to the current problem as it is able to traverse the entire design space with limited risk of becoming trapped in local optima.

Holistic optimisation clearly requires consideration of detailed economic factors (as discussed in section 5), network integration, material limits, and other practical issues that lie outside the

scope of the present paper. Nonetheless, a preliminary indication of useful design trends can be obtained on the basis of thermodynamics and simplified economic considerations by maximising the round-trip efficiency and minimising the capital cost per work output. The round-trip efficiency is defined as the ratio of the net work output during discharge to the net work input during charge. The works are integrated over the periods of operation and include the work required to overcome the various availability losses described in section 3. Thermodynamic inefficiencies in the compression and expansion system are also included, following the methodology of [5, 6]. The round-trip efficiency is a measure of the internal thermodynamic efficiency of the system and does not account inefficiencies in the electrical machines or mechanical losses in the compression-expansion system.

Strictly, the optimiser carries out a minimisation and the objective functions are therefore expressed as

$$f_1 = 1 - \frac{\text{Net work output}}{\text{Net work input}} = 1 - \frac{W_{\text{dis}}}{W_{\text{chg}}} \tag{9}$$

$$f_2 = -\frac{C_{\text{cap}}}{W_{\text{dis}}} \tag{10}$$

Optimal solutions are presented on a Pareto front which illustrates the trade-off surface between different objective functions and allows the designer to study the full range of potential solutions.

The optimisation was formulated for a 2 MW PTES system with a maximum energy storage capacity of 16 MWh. The system was set up to operate on a 24 hour cycle, with the nominal design charging, discharging and storing for eight hours each. There were 11 design variables. For each packed bed there is the aspect ratio L/D, particle diameter d_p, and number of segments N_{seg}. In addition, there is the charging and discharging pressure ratio $\beta_{\text{chg, dis}}$, the temperatures T_1 and T_3 (see figure 1a), and the utilisation or cycle period Π. The nominal design parameters and their minimum and maximum values are given in table 2. Constraints are placed on the value of T_2 and T_4 as specified in table 2. The specifics of applying a multi-objective optimisation algorithm to the PTES system are detailed fully in [6].

Table 2 Parameters varied during optimisation. N_{seg} is the number of segments, T_{1-4} are operating temperatures which correspond to figure 1, β is the charging and discharging pressure ratio, and Π is the utilisation factor or cycle period.

	L/D	d_p (mm)	N_{seg}	T_1 (K)	T_2 (K)	T_3 (K)	T_4 (K)	β	Π
Nominal	1.0	20.0	1	310	773	310	123	10.0	0.75
Minimum	0.1	1.5	1	$T_0 + 10$	$T_3 + 50$	$T_0 + 10$	103	2.0	0.1
Maximum	10.0	50.0	32	473	873	473	$T_1 - 50$	15.0	1.0

In addition, the economic factor k_r was varied as discussed in section 5. The Pareto fronts are shown in figure 6a) and demonstrate the expected trade-off between capital cost and efficiency. A nominal design point is shown for comparison. Design data for the nominal case and for the four emphasised points in figure 6a) are given in table 3.

Analysis of the results suggests that the optimal design varies along the Pareto front. For instance, P2 achieves lower costs than P1 by reducing the pressure ratio, which decreases both the pressure vessel cost and the reciprocating device cost at the expense of efficiency. The change in pressure ratio also affects the temperatures around the cycle. In addition, P2 has a longer cycle

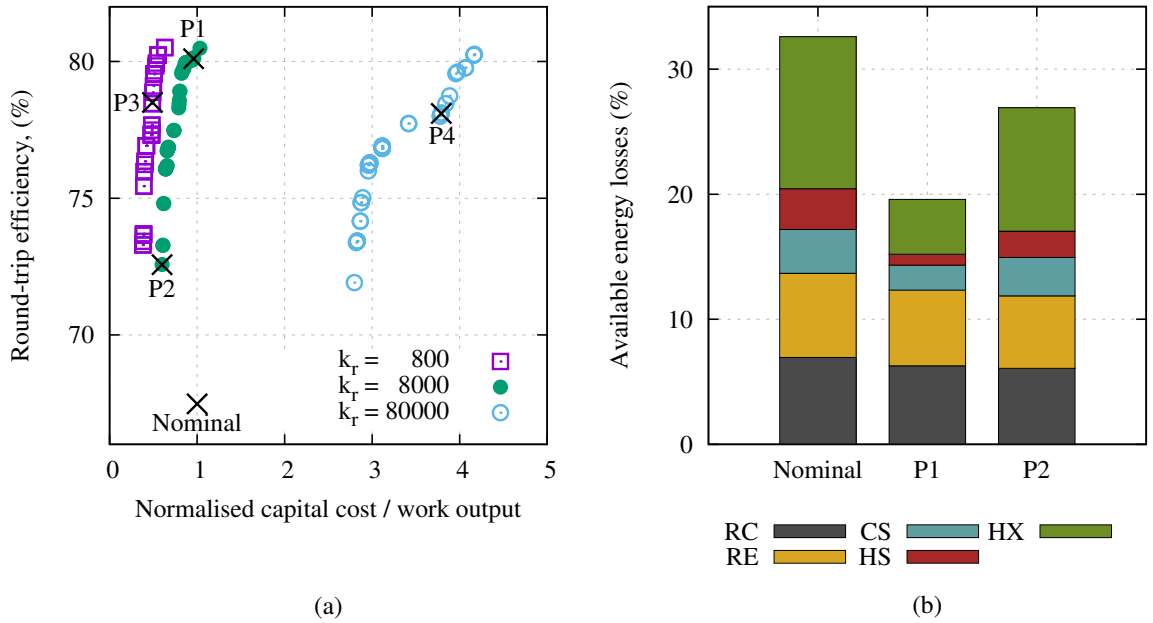

Fig. 6. *Optimisation results*
a) Pareto fronts showing the trade-off between capital cost and round-trip efficiency. Capital cost over work outputs have been normalised by the nominal value. Points P1-P4 are shown in table 3. b) Availability losses in various PTES components for the nominal design, and for P1 and P2. Key: RC reciprocating compressor; RE reciprocating expander; CS cold store; HS hot store; HX heat exchangers

length leading to a greater quantity of energy being stored each cycle, thereby reducing the cost (and efficiency, as described in [6]). These results are consistent with the trends found in previous optimisation studies by McTigue [6].

It is notable that the optimal designs all include segmented packed beds; both hot and cold. A sensitivity analysis showed that the PTES efficiency was not very sensitive to the number of segments in the hot store. In practice the marginal benefit derived from using a segmented hot store will probably be outweighed by the additional complexity and cost of installation that has not been accounted for in this study. On the other hand, the efficiency was sensitive to the number of cold store segments. For instance, evaluating the P1 design with an unsegmented cold store caused the cold store losses to increase from 1.8% to 2.1% i.e. segmentation reduces cold store losses by 14%. It is worth noting that the current PTES set up only allowed quite short storage periods (around eight hours). Given the results of section 4, it is possible that segmentation would have provided a greater benefit if storage occurred for a number of days.

It was noted that while k_r significantly affects the capital cost, it has little influence over the designs that the optimisation routine converges on. This suggests that the PTES design may be robust to variations in component costs, and that these factors have little impact on the final design. Further sensitivity analysis is ideally required.

Figure 6b) compares the availability losses in each component for the nominal design with optimal designs P1 and P2. Compared to the nominal design, P1 significant reduces reservoir losses although there is little change in the reciprocating device losses. Exergetic losses in the

Table 3 Design parameters and performance of the nominal case, and of four optimal solutions that are highlighted in figure 6a).

		Nom.	P1	P2	P3	P4
Hot store	Aspect ratio L/D	1.0	1.74	1.32	1.76	1.98
	Particle diam. d_p (mm)	20.0	2.17	3.95	2.21	2.35
	Segments, N_{seg}	1	28	15	14	30
Cold store	Aspect ratio L/D	1.0	0.52	0.53	0.66	0.62
	Particle diam. d_p (mm)	20.0	4.08	4.08	4.04	4.08
	Segments, N_{seg}	1	25	21	24	24
	T_1 (K)	310.0	316.8	417.4	323.2	317.8
	T_2 (K)	778.0	859.4	868.1	870.2	860.7
	T_3 (K)	310.0	308.5	308.2	308.4	310.0
	T_4 (K)	123.0	118.3	152.6	119.1	119.1
	Charge pressure ratio, β_{chg}	10.0	12.1	6.24	11.9	12.1
	Discharge pressure ratio, β_{dis}	10.0	9.85	5.97	9.84	9.78
	Charging period, Π	0.75	0.66	0.85	0.80	0.81
	Efficiency (%)	67.5	80.1	72.6	78.5	78.1
	Normalised capital cost per work output	1.0	0.96	0.60	0.49	3.79

packed beds are smaller than losses in the compressor and expander. These results were obtained using an 'optimistic' estimation of polytropic efficiency for reciprocating devices of 98%. It has been shown that PTES performance is very sensitive to the polytropic efficiency [5, 6]. If such high values cannot be achieved in practice then it is likely that reciprocating device losses and costs will dominate. In this scenario, although features such as segmentation would improve packed bed performance, the marginal benefit to the full PTES system may be quite small.

7. Conclusions

A Pumped Thermal Energy Storage (PTES) system has been described. Thermal energy is stored in packed-bed thermal reservoirs, and numerous loss mechanisms reduce the exergy content. Careful design of the packed beds can help to minimise these losses. Segmentation of the thermal reservoirs is proposed as a novel design feature which allows smaller particles to be used and consequently increase the efficiency and the energy stored per cycle. Segmentation reduces conductive losses during the storage phase proving that the stores are sufficiently insulated.

The PTES system is optimised with the objectives of maximising round-trip efficiency and minimising capital cost. Pareto fronts illustrate the expected trade-off between these two goals and show that PTES can achieve thermodynamic efficiencies in the region of 70–80% before mechanical and electrical losses are accounted for. The cheapest designs have lower pressure ratios and long cycle durations which lead to lower efficiencies. Optimal designs often feature segmented packed beds, although utilisation of this feature will depend on the additional cost of required equipment (valves, sensors) and the realistic efficiency of the reciprocating devices.

8. Acknowledgement

The work described in this paper was undertaken as part of a project funded by the UK Engineering and Physical Sciences Research Council (EPSRC Grant No. EP/J006246/1). The first author

was supported by an EPSRC-funded studentship and attended the Off-Shore Energy and Storage Conference (OSES) 2015 with the assistance of the Energy Storage Research Network (ESRN). The authors gratefully acknowledge this support.

Nomenclature

c_s	Solid heat capacity, J kg^{-1} K^{-1}	U_s	Wall heat transfer coefficient, W m^{-2} K^{-1}
c_p	Gas isobaric heat capacity, J kg^{-1} K^{-1}	W	Work, J
C	Capital cost, £	V	Volume, m^3
d_p	Particle diameter, m	α	Thermal diffusivity, m^{2}s^{-1}
D	Packed bed diameter, m	β	Heat leakage factor, s^{-1}
G	Mass flow rate per unit area, kg m^{-2}	$\beta_{\text{chg, dis}}$	Pressure ratio
h	Heat transfer coefficient, W m^{-2} K^{-1}	ε	Void fraction
k	Cost factor	Π	Utilisation, cycle period
k_{eff}	Effective conductivity, W m^{-1} K^{-1}	ρ	Density, kg m^{-3}
ℓ	Thermal length scale, m	τ	Thermal time scale, s
L	Packed bed length, m		
N_{seg}	Number of segments	**Subscripts**	
P	Pressure, N m^{-2}	0	Ambient conditions
St	Stanton number	chg, dis	Charge, discharge
S_v	Particle surface to volume ratio, m^{-1}	g, s	Gas, solid
T	Temperature, K	p, i, PV	Packing, insulation, pressure vessel
		r	Reciprocating devices

9. References

[1] DECC: 'DUKES: Digest of United Kingdom Energy Statistics 2014', 2014

[2] Willetts, D.: 'Eight Great Technologies,' (Policy Exchange) 2013

[3] Mackay, D. J. C.: 'Fluctuations and storage', in 'Sustainable Energy – without the hot air', (UIT Cambridge, 2008, 1st edn.) pp. 186–203. Available free online from www.withouthotair.com

[4] MacNaghten, J., Howes, J. S.: 'Energy Storage', patent number WO/2009/044139 A2, 2009

[5] White, A., Parks, G., Markides, C. N.: 'Thermodynamic analysis of pumped thermal electricity storage', Appl. Therm. Eng., 2013, 53, **2**, pp. 291-298

[6] McTigue, J. D., White, A. J., Markides, C. N.: 'Parametric studies and optimisation of pumped thermal electricity storage', Appl. Energy, 2015, 137, pp. 800-811

[7] MacNaghten, J., Howes, J. S., Hunt, R. G.: 'Improved Heat Storage Apparatus', Patent number EP2689207, 2011.

[8] Willmot, A.: 'Dynamics of Regenerative Heat Transfer', (Taylor & Francis, 2002)

[9] White, A. J.: 'Loss analysis of thermal reservoirs for electrical energy storage schemes', Appl. Energy, 2011, 88, **11**, pp. 4150-4159

[10] White, A. J., McTigue, J. D., Markides, C. N.: 'Wave propagation and thermodynamic losses in packed-bed thermal reservoirs for energy storage', Appl. Energy, 2014, 130, pp. 648-657

[11] Wakao, N., Kaguei, S., Funazkri, T.: 'Effect of fluid dispersion coefficients on particle-to-fluid heat transfer coefficients in packed beds', Chem. Eng. Sci., 1979, 34, pp. 325-336

[12] J. Chase, M.W.: 'NIST-JANAF Themochemical Tables, Fourth Edition,' J. Phys. Chem. Ref. Data, 1998, Monogr. 9, pp. 1-1951

[13] Crandall, D. M., Thatcher, E. F.: 'Segmented thermal storage', Sol. Energy, 2004, 77, **4**, pp. 435-440

[14] Granta Design: 'CES Edupack Materials Selector', http://www.grantadesign.com/education/edupack/index.htm, accessed 17/05/2016

[15] Deb, K., Pratap, A., Agarwal, S., Meyarivan, T.: 'A Fast and Elitist Multiobjective Genetic Algorithm: NSGA-II', IEEE Trans. Evol. Comput., 2002 6, **2**, pp. 182-197